PROCEEDINGS OF THE 2nd WORKSHOP ON POSITIONING, NAVIGATION AND COMMUNICATION (WPNC'05)
& 1st ULTRA-WIDEBAND EXPERT TALK (UET'05)

Accuracy of an UWB localization system based on a CMOS chip

Michael TÜCHLER, Volker SCHWARZ, Alexander HUBER

Zentrum für Mikroelektronik Aargau, Fachhochschule Aargau, Schweiz,
e-mail: m.tuechler@zma.ch

Abstract - In this paper, we analyze the achievable location accuracy of a high-precision localization system using time-difference-of-arrival measurements of ultra wide-band (UWB) pulses. This system is under development at our institute and based on a low-power CMOS chip. Similar commercially available localization systems achieve location accuracies (location error standard deviation) down to 15cm under line-of-sight conditions in a working range of 20m indoors (30cm in a 100m range outdoors). We review the fundamental limits of the ranging accuracy of any localization system satisfying the regulatory constraints for UWB emissions. Next, we incorporate realistic characteristics of the UWB radio channel and the CMOS receiver into the analysis. We show that the ranging accuracy is heavily influenced by the available signal-to-noise ratio, i.e., the distance between the antennas, and the multi-path nature of the UWB radio channel. The effect of sampling time jitter of the receiver clock is shown to be negligible. With our proposed system design a ranging accuracy down to 1cm in a working range of 40m can be achieved, which outperforms the accuracy of existing systems.

1 Introduction

An application utilizing the radio channel is commonly called ultra wide-band (UWB), if the covered bandwidth is *>0.5GHz* or *>20%* of the center frequency. Until recently, only niche applications such as radar, sensing, or military communications deserved to be called UWB. This is different today, where numerous companies and university investigate applications using the huge bandwidth of *7.5GHz* in the band from *3.1GHz* to *10.6GHz*. An important milestone to trigger this research was the regulation of how to commercially use this band by the Federal Communications Commission (FCC) [1] or the European Telecommunications Standards Institute (ETSI) [2].
Besides the established companies with know-how in UWB technology such as Time Domain [3], the majority of commercial market players in this area currently focuses on short-range medium- to high-rate communication applications for so-called wireless personal area networks (WPAN). A number of companies already offer chip sets for the WPAN standards IEEE802.15.3a/4a [4;5] implementing the multi-band orthogonal frequency division multiplex (M-OFDM) approach such as [6-9]. This scheme was favored among other proposals such as the direct-sequence spread spectrum scheme from XtremeSpectrum (now Freescale) [10], since the required circuitry for the M-OFDM scheme is more established. Pulse position modulation (PPM) is another method for UWB-based communication proposed by Time Domain [3]. The potential of location and tracking applications has been discussed by the standardization task groups [4;5] as well, but the major industry players currently refrain from large investments in this area, because much higher revenue is in the mass market of the end consumer communication devices. There are quite a few academic groups working on UWB localization solutions as well such as [11-14].
We currently develop hardware for a high-precision localization system based on time-difference-of-arrival (TDOA) measurements of UWB pulses depicted in Figure 1. Using a performance analysis and with simulation results we show that this system achieves a ranging accuracy that is comparable to or even better than that of current state-of-the-art technology in UWB location and tracking. Moreover,

the system complies with the stringent ETSI regulations for UWB emissions. It can cope with signal interference of narrow-band communication services in the *3.1-10.6GHz* band such as the wireless local area network (WLAN) standard IEEE802.11.a. The architecture also promises low power consumption especially for the tags to be localized with the system and can, due to the fully digital signal processing, be easily adapted to several UWB communication standards.
The next section continues with the description of our system proposal. In Section 3 are derived the theoretical limits of the achievable ranging accuracy given perfect and non-perfect receiver circuitry. These limits are compared to simulation results in Section 4. The paper concludes with Section 5.

2 System description

A small tag transmits a sequence of UWB pulses to a set of base stations, which report the arrival time of the pulse train to a processing hub to calculate the tag coordinate *(x,y,z).* This is a so-called time-difference-of-arrival (TDOA) scheme [15]. The system should be able to accommodate a large number of tags to be monitored at the same time. Also, the tags should be able to move in between different "cells", which is a subset of the monitored tag range controlled by at least four base stations.

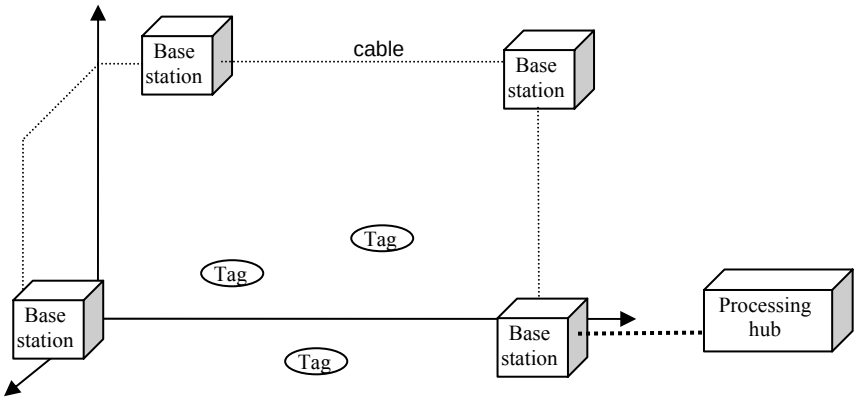

Figure 1: A wireless localization system.

We define the ranging accuracy of a localization system as the standard deviation σ_R of the error

$$e_R = \sqrt{(\hat{x}-x)^2 + (\hat{y}-y)^2 + (\hat{z}-z)^2}$$

between the true tag coordinate *(x,y,z)* and its estimate*.* Commercially available UWB-based systems achieve an accuracy down to σ_R*=15cm* under line-of-sight (LOS) conditions in a working range of up to *50m* outdoors [16] or σ_R*=30cm* (LOS, working range *100m,* outdoors) [17]. In a laboratory environment, σ_R*=10cm* have been reached [3]. The approaches in [18;19] achieve accuracies in the mm or even μm range, but these results are based on transmitting pulses through a calibrated analog delay line and not through a radio channel. The working range and the ranging accuracy decrease indoors due to heavy multi-path scattering and signal losses through walls and objects. Non-LOS (NLOS) conditions (no direct path between tag and base station) severely degrade the location accuracy and are disregarded in the sequel.
For the applications we have in mind, a significantly increased accuracy in the cm or even mm range under LOS both indoors (e.g., office environment) and outdoors (e.g., block of buildings) is required. The desired working range is *20m* indoors and at least *100m* outdoors. Our goal is to determine the location accuracy σ_R for the system. There are numerous factors limiting σ_R such as the characteristics (geometry, aperture, gain, reference point), the radio channel (multi-path propagation, path loss, noise, interference), the receiver circuit (noise figure, bandwidth, sampling rate, sampling, accuracy, clock stability), and the entire system design (base station clock synchronization, algorithm for coordinate

calculation, access control, pulse repetition rate, number of tags).

In the sequel, we focus on the tag and base station circuitry, whose basic building blocks are depicted in Figure 2. The tags should be cheap and have very low power consumption. We realize the entire (tag's) transmitter and the (base station's) receiver circuit on a single chip in CMOS technology. Each base station estimates the pulse travel time T_i between the tag and the *i*-th base station, *i=1,2,3,4,* by processing the received UWB pulse. The tag coordinates *(x,y,z)* follow from the relationship

$$c \cdot (T_i - T_0) = \sqrt{(x - x_i)^2 + (y - y_i)^2 + (z - z_i)^2}, \quad i = 1,2,3,4,$$

where (x_i,y_i,z_i) is the coordinate of the *i*-th base station, *c* is the speed of light, and T_0 is the unknown time when the tag started to send the UWB pulse.

In this paper, we derive lower bounds on the standard deviation σ_T of the time measurement errors

$$e_{T,i} = \hat{T}_i - T_i$$

occurring independently in each base station. We attempt to make our analysis as accurate as possible by covering the most important sources for time measurement errors: thermal noise, timing jitter, and multi-path propagation. These bounds are compared to simulation results aiming to closely model the receiver hardware and the radio channel. To specify the ranging accuracy σ_R from σ_T, the positions of the tag and the base stations as well as the used algorithm to convert the T_i into *(x,y,z)* must be known. Since our focus is on precise time measurement, we apply for simplicity the best-case relationship

$$\sigma_R \geq 2.5 \cdot c \cdot \sigma_T$$

between σ_R and σ_T taken from [15] (p. 183), which holds for small σ_T using the direct calculation of the coordinates *(x,y,z)* from the delays T_i. Similar studies have been conducted in [20-22], but without incorporating regulatory constraints, timing jitter, and multi-path propagation.

Our proposed hardware architecture shown in Figure 2 is based on the proposal in [23]. It establishes a fully digital parallel sampling architecture intended for low-data rate full-band impulse radio UWB. We chose this architecture, because it is suitable for full integration in state-of-the-art CMOS technology, therefore offering a potential low-cost solution at high production volumes. The architecture furthermore offers a great flexibility in terms of the applied signal processing since modulation and demodulation is completely performed by digital circuitry. We concentrate on the location/ranging capability in our work, but integration into a communication system especially at low data rate is certainly possible. The one-bit sampling architecture is most suitable for recovering the received waveform and estimating the impulse response in low signal-to-noise ratios (SNRs), but as shown in Section 4, it works in our application at high SNRs as well. The DLL and phase rotator present in Figure 2 are used for synchronization of the receiver clock and the tag's transmit clock.

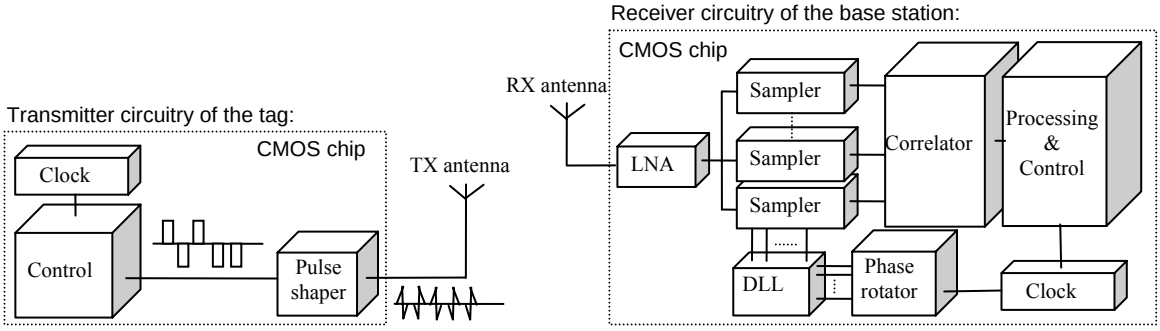

Figure 2: Basic building blocks of the tag's transmitter and the base station's receiver circuitry.

3 Analysis of the time measurement accuracy

Considering the regulatory constraints on UWB emissions imposed by the FCC in the USA [24], the allowed effective isotropically radiated power (EIRP) of our UWB location system is limited by the spectral densities *-34dBm/MHz* (peak) and *-41.3dBm/MHz* (average), which corresponds to a transmit power of *3mW* (peak) and *0.56mW* (average) when the entire spectrum from *3.1* to *10.6GHz* is covered up to the EIRP limit. If a tag transmits the pulse $s_{T,raw}(t)$, then the *i*-th base station receives the pulse

$$s_R(t) = \sqrt{G_{path}} \cdot \left(s_T(t - T_i) + \sum_{k=1}^{\infty} a_k \cdot s_T(t - T_i - \tau_k) \right), \quad s_T(t) = s_{T,raw}(t) * h_{TX}(t) * h_{RX}(t),$$

where G_{path} is the path loss of the channel, $s_T(t)$ is the effective transmit pulse including the impulse responses of the TX and the RX antenna, respectively, and a_k is the coefficient of the *k*-th multi-path component in the radio channel with delay τ_k. To specify the antenna and radio channel characteristics, we work with our industry partners and use results from [15;25;26]. Consider for example the channel measurements in Figure 3, where a UWB pulse was transmitted under clear LOS conditions [27].

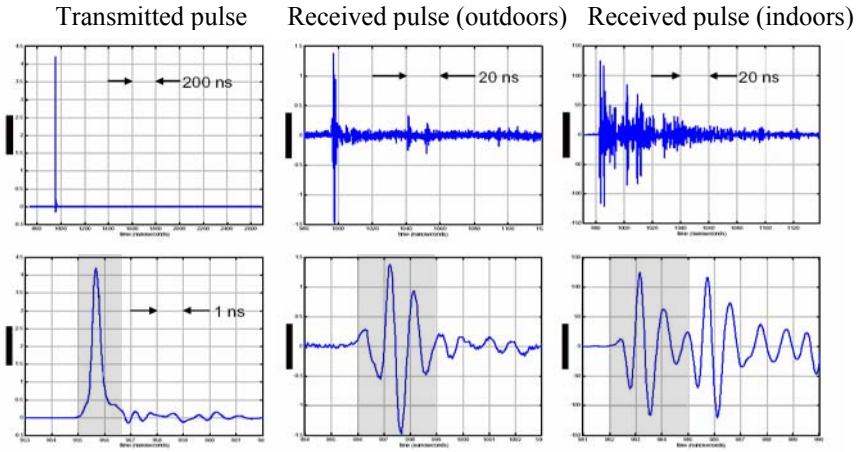

Figure 3: Examples of UWB pulse transmissions under LOS conditions indoors and outdoors.

Our receiver circuitry will perform the measurement of the time delay T_i using the direct component $G_{path}^{1/2} \cdot s_T(t-T_i)$ of $s_T(t)$ in the received pulse $s_R(t)$, only. This component is depicted in the shaded areas in Figure 3. For zero gain TX and RX antennas, the path loss G_{path} is given by

$$G_{\text{path}} = (c / 4\pi f_{cg})^2 \cdot d^{-k_{\text{pl}}},$$

where f_{cg} is the geometric center frequency of the pulse, d is the distance between the antennas, and k_{pl} is the path loss exponent. We chose $k_{pl}=2$ (spherical path loss), which is realistic under a LOS condition without narrow-band interference effects (k_{pl} can be as large as *4*), strong signal scattering ($k_{pl}=3$ indoors), or constructive interference ($k_{pl}<2$) [26]. Since all multi-path components contained in $s_R(t)$ must travel more than the direct distance d, the magnitude of the coefficients a_k is always smaller than 1. The received pulse $s_R(t)$ is amplified with a CMOS wide-band low noise amplifier (LNA) [28] with gain G_{lna} and a noise figure k_{nf} between *2.5* (*4dB* at *4GHz*) and *6.3* (*8dB* at *10GHz*). The total noise power is $P_n=k_{nf}\, N_0\, B_R$, where B_R is the receiver bandwidth of the pulse. The *S* parallel samplers in the base stations are fed from a clock with period T_{clk}, i.e., the effective sampling time is $T_s=T_{clk}/S$. For the analysis of the time measurement error σ_T, we assume first that no timing jitter or multi-path propagation occurs, i.e., the received pulse $s_R(t)$ is given by $G_{path}^{1/2} \cdot s_T(t-T_i)$, which yields the samples

$$s_n = \sqrt{G_{\text{lna}}\, G_{\text{path}}} \cdot s_T(nT_s - T_i) + w_n,$$

where the w_n are Gaussian-distributed noise samples with zero mean and variance σ_W^2. We set B_R to $1/(2T_s)$, such that the noise samples w_n are independent and their variance is given by

$$\sigma_W^2 = P_n = k_{nf} N_0 B_R = k_{nf} N_0 /(2T_s).$$

The smallest possible time measurement error σ_T given the data s_n with any type of signal processing is determined by the Cramer-Rao lower bound

$$\sigma_T(T_i) \geq I_F(T_i)^{-1/2}, \quad I_F(T_i) = \sum_{n=-\infty}^{+\infty} G_{\text{lna}} G_{\text{path}} \cdot \dot{s}_T(nT_s - T_i)^2 / \sigma_W^2, \quad \dot{s}_T(t) = \frac{ds(t)}{dt},$$

where $I_F(T_i)$ is the Fisher information [29] (p. 36). The dependence of $\sigma_T(T_i)$ on the unknown time delay T_i is averaged out by integrating over a time interval of length T_s,

$$\sigma_T = \frac{1}{T_s}\int_0^{T_s} \sigma_T(T_i) dT_i \quad \geq \quad \left(\frac{1}{T_s}\int_0^{T_s} I_F(T_i) dT_i \right)^{-1/2}.$$

The bound follows from the fact that $f(x)=x^{-1/2}$ is a convex function. The integral over $I_F(T_i)$ is given by

$$\frac{1}{T_s}\int_0^{T_s} I_F(T_i) dT_i = \frac{G_{\text{lna}} G_{\text{path}}}{T_s \sigma_W^2} \cdot \int_{-\infty}^{+\infty} \dot{s}_T(t)^2 dt = \frac{G_{\text{lna}} G_{\text{path}} \cdot E_T \cdot (2\pi f_{cq})^2}{T_s \sigma_W^2}, \quad E_T = \int_{-\infty}^{+\infty} s_T(t)^2 dt, \quad f_{cq} = \sqrt{\frac{\int_{-\infty}^{+\infty} f^2 |S_T(f)|^2 df}{\int_{-\infty}^{+\infty} |S_T(f)|^2 df}},$$

where $S_T(f)$ is the spectrum of the transmit pulse $s_T(t)$, E_T is the energy of $s_T(t)$, and f_{cq} is the quadratic center frequency of $S_T(f)$, which can be approximated by the (smaller) geometric center frequency f_{cg}. Plugging in the expressions for G_{path} and σ_W^2 yields

$$\sigma_T \geq \sqrt{2 \cdot \frac{d^{k_{\text{pl}}}}{c^2} \cdot \frac{1}{G_{\text{lna}}} \cdot \frac{k_{nf} N_0}{E_T}}.$$

The time measurement accuracy improves with a high SNR $E_T/(k_{nf}N_0)$ and a large amplitude of the received signal $s_R(t)$ (large G_{lna}). The gain in accuracy from fast changes in the transmit pulse $s_T(t)$ over time (large f_{cq}) is cancelled by the decreasing antenna aperture (large f_{cg} in G_{path}). It follows that the accuracy of a wireless localization system without time jitter and multi-path propagation is basically determined by the available SNR.

We continue our analysis by incorporating time jitter as well, i.e., the samples s_n are given by

$$s_n = \sqrt{G_{\text{lna}} G_{\text{path}}} \cdot s_T(nT_s + j_n - T_i) + w_n,$$

where j_n is a Gaussian-distributed sampling time jitter independent over the index n with zero mean and standard deviation σ_J. We set σ_J to *10ps* for the chosen CMOS technology. Note however that there exist CMOS phase locked loops with root-mean-square (RMS) jitter values down to *0.8ps* for clock generation [30] and clock/data recovery circuits at *10GBit/s* [31].

The time jitter noise translates into amplitude noise using a first-order Taylor approximation of $s_T(t)$,

$$s_n = \sqrt{G_{\text{lna}} G_{\text{path}}} \cdot \left(s_T(nT_s - T_i) + \dot{s}_T(nT_s - T_i) \cdot v_n \right) + w_n, \quad \dot{s}_T(t) = d\, s_T(t) / dt,$$

where the v_n are Gaussian-distributed noise samples with zero mean and variance σ_J^2. The time measurement error σ_T is now lower bounded as follows:

$$\sigma_T(T_i) \geq I_F(T_i)^{-1/2}, \quad I_F(T_i) = \sum_{n=-\infty}^{+\infty} G_{\text{lna}} G_{\text{path}} \cdot \dot{s}_T(nT_s - T_i)^2 / (\sigma_W^2 + G_{\text{lna}} G_{\text{path}} \sigma_J^2 \cdot \dot{s}_T(nT_s - T_i)^2).$$

Assuming that the addends in the sum are non-zero only at Z indices n from the set Ω, we can write

$$I_F(T_i) = \frac{Z}{Z} \cdot \sum_{n \in \Omega} \frac{1}{\sigma_W^2 / \left(G_{\text{lna}} G_{\text{path}} \dot{s}_T(nT_s - T_i)^2 \right) + \sigma_J^2} \leq \frac{1}{\sigma_W^2 / \left(G_{\text{lna}} G_{\text{path}} \Sigma_{n \in \Omega} \dot{s}_T(nT_s - T_i)^2 \right) + \sigma_J^2 / Z}.$$

The bound follows from the fact that $f(x)=1/(x^{-1}+1)$ is a concave function. We again integrate $\sigma_T(T_i)$ over an arbitrary time interval of length T_s yielding

$$\sigma_T = \frac{1}{T_s}\int_0^{T_s} \sigma_T(T_i) dT_i \quad \geq \quad \left(\sigma_W^2 / \left(G_{\text{lna}} G_{\text{path}} \frac{1}{T_s}\int_0^{T_s} \Sigma_{n \in \Omega} \dot{s}_T(nT_s - T_i)^2 dT_i \right) + \sigma_J^2 / Z \right)^{1/2}.$$

The bound follows from the fact that $f(x)=(x^{-1}+1)^{1/2}$ is a convex function. The above expression simplifies as by plugging in the expressions for G_{path} and σ_W^2:

$$\sigma_T \geq \left(T_s \sigma_W^2 / \left(G_{\text{lna}} G_{\text{path}} \int_{-\infty}^{+\infty} \Sigma_{n\in\Omega} \dot{s}_T(t)^2 dt \right) + \sigma_J^2 / Z \right)^{1/2} = \sqrt{2 \cdot \frac{d^{k_{\text{pl}}}}{c^2} \cdot \frac{1}{G_{\text{lna}}} \cdot \frac{k_{nf} N_0}{E_T} + \frac{\sigma_J^2}{Z}}.$$

The only difference to the jitter-free case is the extra term σ_J^2/Z. As shown in Section 4, for the parameter setting in our application, the effect of (independent) time jitter on the ranging error is negligible. For larger σ_J^2, the effect of time jitter is in general reduced with a higher sampling frequency (yielding a larger Z), which reduces the term σ_J^2/Z in the above equation for σ_T.

In the sequel, we assume that a train of P pulses $s_T(t)$ is transmitted, which yields the following improved ranging error provided that the tag and the base station clock are perfectly synchronized:

$$\text{without jitter}: \sigma_T \geq \frac{1}{\sqrt{P}} \cdot \sqrt{\frac{d^{k_{\text{pl}}}}{c^2} \cdot \frac{2}{G_{\text{lna}}} \cdot \frac{k_{nf} N_0}{E_T}}, \qquad \text{with jitter}: \sigma_T \geq \frac{1}{\sqrt{P}} \cdot \sqrt{\frac{d^{k_{\text{pl}}}}{c^2} \cdot \frac{2}{G_{\text{lna}}} \cdot \frac{k_{nf} N_0}{E_T} + \frac{\sigma_J^2}{Z}}.$$

Until now we assumed that the samples s_n are continuous-valued. However, we apply digital signal processing in the receiver, which requires quantizing them. Doing this with high accuracy is an area and power consuming task on the CMOS chip, in particular at the sampling frequency we consider. We thus proceed with the analysis when 1Bit-quantization is applied, i.e., the samples s_n are given by

$$s_n = q(\sqrt{G_{\text{lna}} G_{\text{path}}} \cdot s_T(nT_s + j_n - T_i) + w_n),$$

where $q(x)=1$ if $x \geq 0$ and $q(x)=0$ if $x<0$. Let T_p be the repetition period of the P transmit pulses $s_T(t)$. The samples s_n are accumulated in an array of $R=T_p/T_s$ registers r_k, whose content is given by

$$r_k = \sum_{n=0}^{P-1} s_{k+nR}.$$

In this model, the sampler in the receiver fed the registers only about P time periods of length T_p. The register content is a random variable with the following mean and variance,

$$E(r_k) = Q(-\sqrt{G_{\text{lna}} G_{\text{path}}} \cdot s_T(kT_s - T_i)/\sigma), \qquad \sigma^2 = \sigma_W^2 + G_{\text{lna}} G_{\text{path}} \sigma_J^2 \cdot \dot{s}_T(nT_s - T_i)^2,$$

$$Var(r_k) = E(r_k) \cdot (1 - E(r_k))/P,$$

where $Q(x)$ is the integral over the function $f(z)=\exp(-z^2/2)/(2\pi)^{1/2}$ from x to ∞. The time measurement error σ_T follows as usual from the Fisher information $I_F(T_i)$:

$$I_F(T_i) = \sum_{k=0}^{R} \exp(-G_{\text{lna}} G_{\text{path}} s_T(kT_s - T_i)^2 / (2\sigma^2))^2 / (2\pi) \cdot G_{\text{lna}} G_{\text{path}} \dot{s}_T(kT_s - T_i)^2 / \sigma^2 / Var(r_k).$$

This expression follows by taking the sum over the squared time derivatives of $E(r_k)$ divided by the noise variance $Var(r_k)$. Also, we assume that the r_k are Gaussian distributed. For small SNRs (large σ_W^2), the argument of the exponential expression in the above equation is well approximated by the constant 1 and the variance $Var(r_k)$ is close to its maximum $1/(4P)$ for all k:

$$I_F(T_i) = \sum_{k=0}^{R} P \cdot \frac{2}{\pi} \cdot G_{\text{lna}} G_{\text{path}} \dot{s}_T(kT_s - T_i)^2 / \sigma^2.$$

This expression is familiar to the second case in our analysis (time jitter and continuous-valued samples s_n) provided that the repetition period T_p is longer that the duration of $s_T(t)$, i.e., there is no overlap. Thus, the same techniques for finding a lower bound on σ_T can be applied, yielding:

$$\sigma_T \geq \frac{1}{\sqrt{P}} \cdot \sqrt{\frac{\pi}{2}} \cdot \sqrt{2 \cdot \frac{d^{k_{\text{pl}}}}{c^2} \cdot \frac{1}{G_{\text{lna}}} \cdot \frac{k_{nf} N_0}{E_T} + \frac{\sigma_J^2}{Z}}.$$

At low SNR, it is sufficient to use 1-Bit quantization, since the time measurement error σ_T degrades only about $(\pi/2)^{1/2}-1=25\%$ compared to using continuous-valued samples s_n. This is not surprising, since a multi-bit quantization of s_n would only more accurately resolve the noise contained in s_n.

As shown in Figure 5, the Cramer-Rao analysis predicts that a properly calibrated wireless localization system can achieve time measurement accuracies in the sub-picosecond range even if there is random time jitter in the sampling times and by applying 1Bit quantization. It turned out that for zero gain

antennas, the actual center frequency (f_{cq} or f_{cg}) of the transmit pulse and the sampling frequency $1/T_s$ do not affect the ranging accuracy considerably.
However, this result holds only by not taking the multi-path effects of the wireless channel into account. The researchers in [32;33] investigate the effects of multi-path propagation on the accuracy on time of arrival (TOA) measurements. They also derive algorithms for estimating the channel impulse response (CIR), which is in our setup a function of the coefficients a_k and the delays τ_k, to improve the measurement accuracy. The problem arising now is that the delays τ_k and, thus, the "delay" $\tau_0=T_i$ of the direct path cannot be estimated at any SNR with a higher resolution than $1/T_s$. This can be modeled as a time jitter on the estimate of T_i and τ_k, which is uniformly distributed in the interval $-1/(2T_s)$ to $+1/(2T_s)$. We found the error in the direct path to be identical for a wide range of UWB channel measurements under LOS conditions such as those depicted in Figure 4, i.e., the error can possibly be corrected by calibration. The true advantage of an UWB localization system is therefore the capability to sound the channel over a wide frequency range to get a fine time resolution of the CIR. Since we do not employ signal processing for estimating the channel impulse response, it is even more important to sample the received signal at a high rate to separate the direct component (with systematic delay error) in the CIR from the multi-path components (with random delay error). Even in case the CIR is estimated, e.g., to improve the SNR, a precise time delay measurement requires to estimate a_k and τ_k precisely as well, which again calls for a high sampling rate.

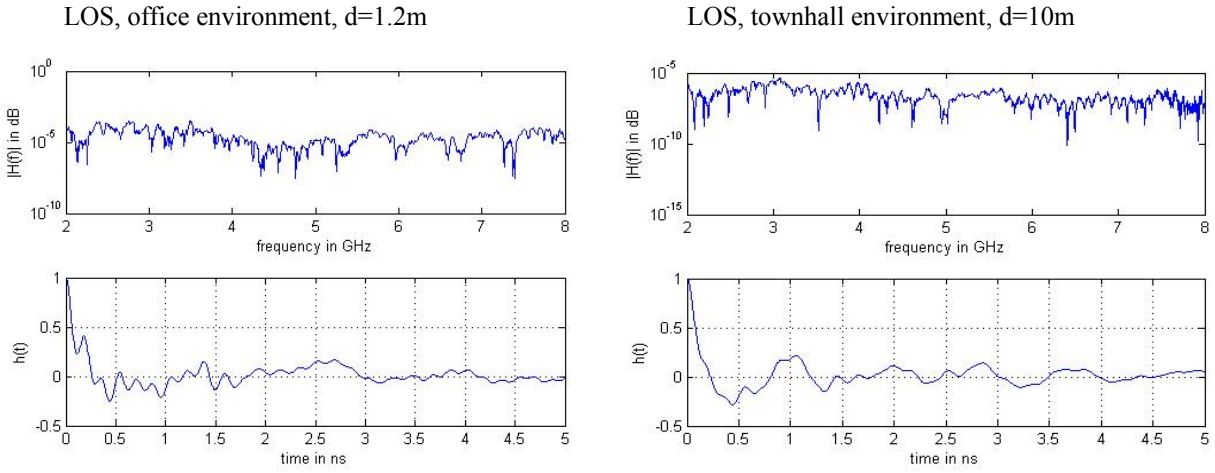

Figure 4: Spectrum and impulse response of two example radio channels. The measurements were taken from the Intel UWB database in [12].

4 Results

Consider the following experimental setup. The transmit pulse $s_T(t)$ is a Gaussian pulse with bandwidth $B=2GHz$ modulated with a cosine of frequency $f_c=4GHz$ and peak transmit power $P_t=0.8mW$. This power attains the regulatory EIRP maximum of $-34dBm/MHz$ by 92%. The pulse repetition time T_p is $100ns$. The tag generates a train of $P=100$ pulses every second, which results in an average power of at most $-90dBm/MHz$ at $4GHz$. This is way below the regulatory limit of $-41dBm/MHz$.The receiver is specified by $k_{nf}=2.5$, $T_{clk}=1GHz$, $S=10$, $G_{lna}=10$, and $\sigma_J=10ps$.
The Cramer-Rao lower bounds on the time measurement error σ_T are shown in Figure 5 as function of the distance d between the TX and RX antenna. The simplified formulas for determining the Cramer Rao bound still give meaningful results. Note that for this analysis (no multi-path effects in the channel) the actual pulse shape or the pulse spectrum have little effect on σ_T, i.e., the results apply to

"real world" pulse shapes as well. From Figure 5 follows that a properly calibrated localization system can achieve a ranging error σ_R of at most $2.5 \cdot c \cdot \sigma_T = 2.5 \cdot c \cdot 1.1ps = 0.83mm$ up to a distance of $d=50m$ between the RX and TX antenna.

The theoretical bounds are compared to simulation results in Figure 6. They were obtained by modeling the UWB transmission and the receiver circuit as defined in the previous sections. For determining the delay T_i, maximum likelihood estimation was applied [29]. A problem turned out to be the synchronization between the tag and base station clock. We assumed that there is initially a $\pm 20ppm$ random clock skew, which after synchronization went down to $1ppm$. For distances larger than $30m$, synchronization sometimes failed, which leads to the jump in σ_T in Figure 6. This part of the receiver circuit is subject to further optimization. Multi-path effects are taken into account by convolving the transmit pulse with measured channel impulse responses (LOS conditions indoors and outdoors, see for example Figure 4) taken from [12].

The simulation results show a significantly higher measurement error σ_T than that predicted by the bounds in Figure 5, but the relative performance between the 3 considered cases (with or without time jitter, 1Bit quantization) is as predicted by the analysis. The multi-path effects influence the standard deviation σ_T of the time measurement error only little. However, as mentioned in Section 3, we observed a systematic excess delay of about $44ps$ in estimating T_i. This delay can easily removed in a real system using proper calibration.

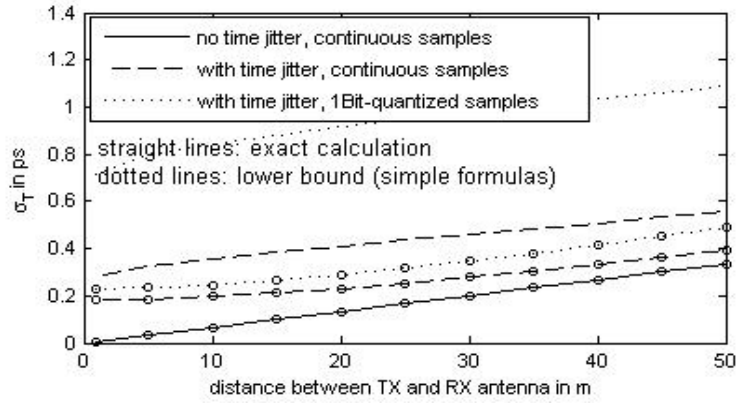

Figure 5: Cramer-Rao lower bounds on the time measurement error σ_T for determining the arrival time of UWB pulses transmitted over a wireless channel. Multi-path effects are not addressed, but sampling time jitter and 1-Bit quantization in the receiver is taken into account.

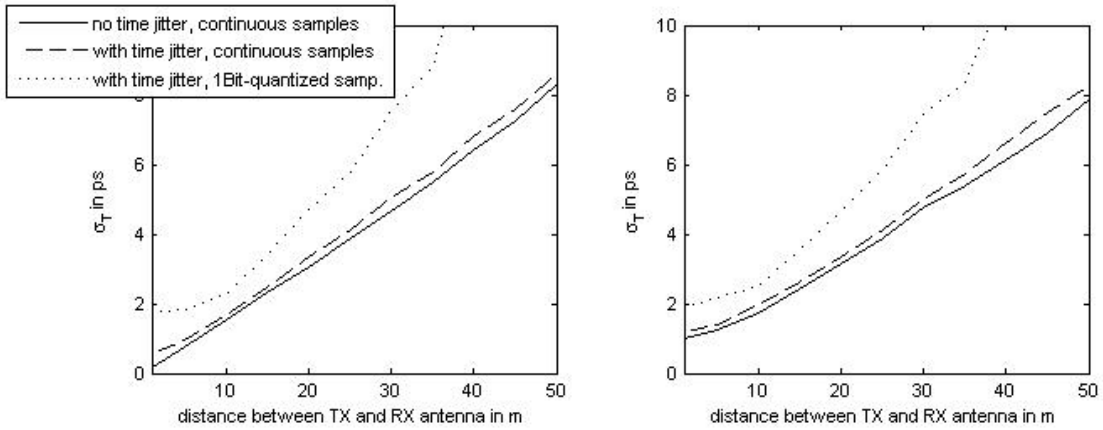

Figure 6: Simulation of the time measurement error σ_T for determining the arrival time of UWB pulses transmitted over a wireless channel, including sampling time jitter and 1-Bit quantization in the receiver circuit. Multi-path effects are taken into account by convolving the transmit pulse with measured CIRs.

5 Discussion

The analysis and the simulation results presented in this paper indicate the following: our hardware design for a localization system based on TDOA measurements of UWB pulses is capable of determining the pulse arrival time with a measurement error of *10ps* in a working range of *40m* under LOS conditions. This corresponds to a ranging accuracy of *1cm* for optimally positioned base stations and assuming a perfect synchronization of the clocks in all the base stations. The underlying simulation providing this result took multi-path effects, sampling time jitter, and 1Bit quantization into account. It turned out that using UWB pulses as such allows precise TOA measurements, but the gain in accuracy is compensated by a smaller receiver SNR, i.e., the pulse bandwidth and center frequency are not the major factor determining the ranging accuracy. However, this finding holds only for pulse transmission over a frequency-flat channel. Given the characteristics of a real-world radio channel, a high pulse bandwidth as well as a high sampling rate is required to obtain the CIR with high resolution. This is necessary the separate the direct component from the (random) multi-path components in the CIR. An attempt to estimate this amplitude and the delays of the multi-path components to improve the SNR and, thus, the time measurement, requires a high sampling rate as well. We conclude that a high-precision wireless localization system must use a high rate sampler in the receiver, i.e., our proposal is a viable candidate for such a system.

6 References

[1] FCC, F. C. C. "Ultra-Wideband Operations FCC Report and Order". Vol. US 47 CFR Part15. 22-4-2002. Federal Communications Commission.

[2] Directorate General of the European Commission. "ETSI, Harmonized Standards Covering Ultrawide Band (UWB) Applications". Vol. DG ENTR/G/3M/329. 25-2-2003.

[3] Time domain Corporation, "Time domain - The Pulse of the Future", http://www.timedomain.com, Last update: 16-12-2004

[4] Institute for Electronics and Electrical Engineers, "IEEE 802.15 WPAN Low Rate Alternative PHY Task Group 4a (TG4a)", www.ieee802.org/15/pub/TG4a.html, Last update: 20-12-2004

[5] Institute for Electronics and Electrical Engineers (IEEE), "IEEE 802.15 WPAN High Rate Alternative PHY Task Group 3a (TG3a)", www.ieee802.org/15/pub/TG3a.html, Last update: 2004

[6] General Atomics, "General Atomics UWB Solutions", http://photonics.ga.com/uwb/index.html, Last update: 2004

[7] PulseLINK, Inc., "PulseLINK", www.pulse-link.net, Last update: 2004

[8] Staccato Communications, "Staccato Communications Wireless USB", www.staccatocommunications.com, Last update: 2004

[9] Wisair, "Wisair UWB chip sets", www.wisair.com, Last update: 2004

[10] Freescale Semiconductor, "Freescale UWB Technology", http://www.freescale.com/UWB, Last update: 2004

[11] University of California at Berkeley, "Berkeley Wireless Research Center", bwrc.eecs.berkeley.edu, Last update: 2004

[12] University of Southern California, "UltraLab for UWB Research", ultra.usc.edu/New_site/database.html, Last update: 2004

[13] Virginia Polytechnic Institute and State University, "UWB Research at the Virginia Tech",

www.ee.vt.edu/~ha/research/uwb/, Last update: 2004

[14] University of Oulu, Finnland, "Center for Wireless Communication", http://www.cwc.oulu.fi/home/, Last update: 2004

[15] Oppermann, I., Hämäläinen, M., and Iinatti, J., *UWB Theory and Applications* Wiley, 2004.

[16] Ubisense Ltd., "Ubisense - The Smart Space Company", http://www.ubisense.net, Last update: 13-12-2004

[17] Multispectral Solutions Inc, "Multispectral Solutions Inc.- A Tradition of Excellence in Innovation", http://www.multispectral.com, Last update: 10-12-2004

[18] Adams, J. C., Gregorwich, W., Capots, L., and Liccardo, D. "Ultra-wideband for navigation and communications". Vol. 2, pp. 2-785-2/792. 2001. *Aerospace Conference, 2001, IEEE Proceedings.*

[19] Zetik, R., Sachs, J., and Thomä, R. "Positioning by means of 5GHz UWB Radar ". pp. 1-9. 2003. *48. Internationales Wissenschaftliches Kolloquium* .

[20] Chung, W. C. and Ha, D. S. "An Accurate Ultra Wideband (UWB) Ranging for Precision Asset Location". pp. 389-393. 2003. *Ultra Wideband Systems and Technologies, 2003 IEEE Conference on*. 16-11-2003.

[21] Catovic, A. and Sahinoglu, Z. "The Cramer-Rao Bounds of Hybrid TOA/RSS and TDOA/RSS Location Estimation Schemes". Vol. TR-2003-143. 1-1-2004. Mitsubishi Electric Research Laboratory.

[22] Lovelace, W. M. and Townsend, J. K. "The effects of timing jitter on the performance of impulse radio". pp. 251-254. 2002. *Ultra Wideband Systems and Technologies, 2002. Digest of Papers. 2002 IEEE Conference on*.

[23] Smaini, L. and Helal, D. "Flexible pulse-based UWB RF transceiver". Vol. 2 (Visuals Supplement), pp. 665-668. 2004. *Solid-State Circuits, International Conference on, Digest of papers*. 15-2-2004.

[24] Federal Communications Commission. "Ultra-Wideband Operations FCC Report and Order". Vol. US 47 CFR Part15. 22-4-2002. Federal Communications Commission.

[25] Fontana, R., "Recent system applications of short-pulse ultra-wideband (UWB) technology," *Microwave Theory and Technology, IEEE Transactions on*, vol. 52, no. 9, pp. 2087-2104, Sept.2004.

[26] Siwiak, K. and McKeown, D., *Ultra-Wideband radio technology* Wiley, 2004.

[27] Scholtz, R. "Short Short-Range Ultra Range Ultra-Wideband Systems". 2004. University of Southern California.

[28] Bevilacqua, A. and Niknejad, A. "An Ultra-Wideband CMAS LNA for 3.1 to 10.6 GHz Wireless Receivers". pp. 382-383. 2004. *IEEE International Solid-State circuits conference*. 2004.

[29] Kay, S., *Fundamentals of Statistical Signal Processing, Estimation Theory* Prentice Hall, 1993.

[30] Da Dalt, N. and Sandner, C., "A subpicosecond jitter PLL for clock generation in 0.12-/spl mu/m digital CMOS," *Solid-State Circuits, IEEE Journal of*, vol. 38, no. 7, pp. 1275-1278, July2003.

[31] Savoj, J. and Razavi, B., "A 10-Gb/s CMOS clock and data recovery circuit with a half-rate binary phase/frequency detector," *Solid-State Circuits, IEEE Journal of*, vol. 38, no. 1, pp. 13-21, Jan.2003.

[32] Lee, J.-Y. and Scholtz, R. A., "Ranging in a dense multipath environment using an UWB radio link," *Selected Areas in Communications, IEEE Journal on*, vol. 20, no. 9, pp. 1677-1683, 2002.

[33] Li, X. and Pahlavan, K., "Super-resolution TOA estimation with diversity for indoor geolocation," *Wireless Communications, IEEE Transactions on*, vol. 3, no. 1, pp. 224-234, Jan.2004.